Excited-State Proton Transfer through Water Bridges and Structure of Hydrogen-Bonded Complexes in 1 H -Pyrrolo[3,2- h]quinoline: Adiabatic Time-Dependent Density Functional Theory...

ARTICLE *in* THE JOURNAL OF PHYSICAL CHEMISTRY A · NOVEMBER 2006

Impact Factor: 2.69 · DOI: 10.1021/jp063426u · Source: PubMed

2 AUTHORS:

Alexander Kyrychenko
V. N. Karazin Kharkiv National University
66 PUBLICATIONS **877** CITATIONS
SEE PROFILE

J. Waluk
Polish Academy of Sciences
254 PUBLICATIONS **3,669** CITATIONS
SEE PROFILE

Excited-State Proton Transfer through Water Bridges and Structure of Hydrogen-Bonded Complexes in 1*H*-Pyrrolo[3,2-*h*]quinoline: Adiabatic Time-Dependent Density Functional Theory Study

A. Kyrychenko[†] and J. Waluk*

Institute of Physical Chemistry, Polish Academy of Sciences, Kasprzaka 44, 01-224 Warsaw, Poland

Received: June 2, 2006; In Final Form: August 24, 2006

Proton transfer reaction is studied for 1*H*-pyrrolo[3,2-*h*]quinoline−water complexes (PQ−$(H_2O)_n$, $n = 0-2$) in the ground and the lowest excited singlet states at the density functional theory (DFT) level. Cyclic hydrogen-bonded complexes are considered, in which water molecules form a bridge connecting the proton donor (pyrrole NH group) and acceptor (quinoline nitrogen) atoms. To understand the effect of the structure and length of water bridges on the excited-state tautomerization in PQ, the potential energy profile of the lowest excited singlet state is calculated adiabatically by the time-dependent DFT (TDDFT) method. The $S_0 \rightarrow S_1$ excitation of PQ is accompanied by significant intramolecular transfer of electron density from the pyrrole ring to the quinoline fragment, so that the acidity of the N−H group and the basicity of the nitrogen atom of the quinoline moiety are increased. These excited-state acid−base changes introduce a driving force for the proton transfer reaction. The adiabatic TDDFT calculations demonstrate, however, that the phototautomerization requires a large activation energy in the isolated PQ molecule due to a high energy barrier separating the normal form and the tautomer. In the 1:1 cyclic PQ−H_2O complex, the energy barrier is dramatically reduced, so that upon excitation of this complex the tautomerization can occur rapidly in one step as concerted asynchronous movements of the two protons assisted by the water molecule. In the PQ−$(H_2O)_2$ solvate two water molecules form a cyclic bridge with sterically strained and unfavorable hydrogen bonds. As a result, some extra activation energy is needed for initiating the proton dislocation along the longer hydrogen-bond network. The full tautomerization in this complex is still possible; however, the cooperative proton transfer is found to be highly asynchronous. Large relaxation and reorganization of the hydrogen-bonded water bridge in PQ−$(H_2O)_2$ are required during the proton translocation from the pyrrole NH group to the quinoline nitrogen; this may block the complete tautomerization in this type of solvate.

Introduction

Heteroazaaromatic molecules containing both hydrogen-bonding donor and hydrogen-bonding acceptor groups are often characterized by rich and complex spectroscopy. One of the most intriguing features is the dual fluorescence revealed in alcohol solutions. This phenomenon has been attributed to phototautomerization, which, formally, corresponds to the proton being translocated from the donor to the acceptor group. It has been found, however, that due to the large spatial separation between the functional groups this phototautomerization cannot occur directly. In such a situation, proton transfer is still possible when assisted by an appropriate protic partner acting simultaneously as a proton donor and an acceptor. Excited-state double proton transfer (ESDPT) has been discovered by Kasha and coworkers[1] for 7-azaindole (7AI) in alcohol complexes and in a doubly hydrogen-bonded dimer formed in high concentrations in nonpolar solvents. Since then, the photophysics of bifunctional compounds composed of pyrrole and pyridine moieties has received a great deal of attention,[2−8] because these biologically relevant molecules can be used as probes in studying protein structure and dynamics due to their high sensitivity to solvent and environment.[9]

1*H*-Pyrrolo[3,2-*h*]quinoline (PQ) and structurally related bifunctional compounds reveal dual fluorescence in alcohols[10−13] and water.[14] The long-wavelength emission band has been attributed to the proton transfer tautomer fluorescence resulting from ESDPT catalyzed by a solvent bridge. The proposed mechanism of a solvent-mediated ESDPT reaction for PQ in protic solvents is, however, quite different from that of 7AI. In the latter, solvent relaxation around an excited 7AI chromophore is found to be necessary to occur prior to ESDPT. For PQ it has been proposed that two different types of population of H-bonded solvates exist in protic solvents already in the ground state. A fraction of "properly" H-bonded species undergoes a fast, femtosecond-scale proton transfer reaction leading to the fluorescent tautomer. Another fraction, consisting of "incorrectly" H-bonded complexes, is deactivated via an efficient nonradiative internal conversion channel to the ground state during solvent rearrangement around an excited chromophore. Molecular dynamics (MD) simulations of the structure of H-bonded complexes in bulk methanol and water, as well as in dilute hydrocarbon solutions with small amounts of these solvents, have demonstrated that the topology of hydrogen-bond donor (pyrrole NH group) and acceptor (pyridine N atom) centers in PQ favors the formation of 1:1 cyclic, doubly H-bonded complexes with alcohols and water.[15] According to the MD results,[15,16] the equilibrium fraction of the 1:1 cyclic H-bonded species in the ground state in bulk methanol is estimated to be ∼1% and ∼70% for 7AI and PQ, respectively. The existence of two populations of H-bonded species of PQ

[†] Permanent address: Research Institute for Chemistry, V.N. Karazin Kharkov National University, 4, Svobody Sq., 61077 Kharkov, Ukraine.

10.1021/jp063426u CCC: $33.50
Published on Web 10/06/2006

deactivated by different ESDPT and nonproton transfer mechanisms has also been successfully proven in a subpicosecond fluorescence upconversion study.[17]

Understanding the mechanism of excited-state proton transfer through a solvent bridge requires knowledge of the structure of H-bonded species. Experimental investigations of the mechanism are possible for small clusters isolated in supersonic jet conditions. These experiments can, in principle, provide detailed information concerning the stoichiometry, geometry, and energetics of different H-bonded complexes. A solvent-assisted proton transfer reaction involves cooperative migration of several protons; therefore, the knowledge of the structures of possible intermediates and transition states along a reaction path enables also understanding of different photoreactivities and kinetics of proton transfer in differently solvated species. Therefore, these studies should be assisted by ab initio or density functional theory calculations. Recently, the proton transfer reaction has been computationally studied for 7AI−$(H_2O)_n$ complexes in both the ground and excited states.[18−24] The reaction path for double and triple proton transfer in cyclic 1:1 and 1:2 water complexes has been considered at different theory levels. The phototautomerization assisted by water bridges has also been theoretically studied for 2-hydroxypyridine[25] and uracil.[26] 7-Hydroxyquinoline (7HQ) is another example of the molecule in which phototautomerization is assisted by a hydrogen-bond network.[27] It has been shown that in 7HQ the excited-state proton transfer may occur through alcohol,[28,29] water,[30] and ammonia[31−33] bridges. Systematic experimental and ab initio studies of 7HQ−$(NH_3)_n$ ($n = 1-6$) have allowed the authors to determine the critical cluster size and to identify the structure of H-bonded solvates enabling proton transfer via an ammonia wire.[34,35]

The purpose of this work is to study the proton transfer reaction in PQ−$(H_2O)_n$ complexes ($n = 0-2$) in the lowest excited singlet state. The results of the molecular dynamics simulations have shown[15] that H-bonded complexes of 1:1 and 1:2 stoichiometries are dominant in bulk methanol and water solutions in the ground state. Therefore, detailed knowledge of the ground-state structure of these H-bonded species is necessary prior to modeling an excited-state tautomerization. In this paper we explore the energetics and the mechanism of proton transfer through a water bridge. To examine the reaction path leading from the normal form (N) to the tautomer (T) via the corresponding transition state (TS), the structure of these stationary points is fully optimized in the lowest excited singlet state by applying the adiabatic time-dependent density functional theory (TDDFT) method.[36] The structure of the transition states and the energy barriers along the proton transfer coordinates are analyzed to understand the photoreactivity of H-bonded species of PQ. The back proton transfer, leading to the recovery of the normal form, is also analyzed for the ground electronic state. A key point of the study is to compare different H-bonded solvates of PQ with water molecules in terms of photoreactive ability to undergo a water-catalyzed proton transfer reaction in the lowest excited singlet state. Finally, possible mechanisms for competitive nonradiative deactivations of photoexcited PQ solvates to the ground state via the internal conversion channel are discussed.

Computational Details

The geometry of isolated PQ and that of PQ−$(H_2O)_n$ complexes in the ground state (S_0) and the lowest electronic excited singlet state (S_1) were optimized using the density functional theory (DFT) method.[37] The equilibrium excited-state structure, dipole moments, and vibrational frequencies were calculated using the time-dependent generalization of the density functional theory method, referred to as TDDFT, with analytical excited-state gradients.[36] The transition states along the proton transfer coordinate on the S_0 and S_1 surfaces were also analyzed. For each optimized structure, harmonic frequencies were evaluated by numerical force constant calculation in order to confirm a true local minimum or a transition state. The vertical electronic singlet and triplet excitation energies, oscillator strengths, and transition moments were also calculated within the TDDFT formalism. The correlation-consistent polarized valence cc-pVDZ basis set[38] was used. The aug-cc-pVDZ basis set was added on each of the two N1 and N4 atoms and the pyrrole hydrogen atom H5 of PQ (Figure 1). In the case of H-bonded water complexes, the aug-cc-pVDZ basis set was also added on all atoms of water molecules. Although valence states were a main interest in the present study, the use of diffuse basis functions is required to describe correctly low-lying Rydberg states as well as $\pi\sigma^*$ excited states. The accurate estimation of energies of these excited states is expected to be important for obtaining reliable results for the photophysics of indole-based molecules.[39,40] Most calculations were done with the hybrid B3LYP functional.[41] Some excitation energies were alternatively calculated at the second-order approximate coupled-cluster (CC2) method employing the resolution-of-the-identity (RI) approximation for the electron repulsion integrals.[42,43] The TURBOMOLE program package, version 5.7,[44] has been used for all calculations.

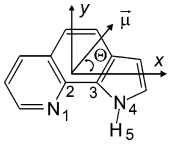

Figure 1. Structure and atom labeling of 1*H*-pyrrolo[3,2-*h*]quinoline (PQ). The arrow defines a positive angle Θ of the direction of the excited-state transition moments and, also, the ground and excited-state permanent dipole moments μ with respect to the long molecular axis *x*.

Results

PQ Monomer. The ground-state geometry of PQ was optimized by means of the DFT method using the hybrid B3LYP functional and the augmented cc-pVDZ basis set as described above. Normal (N) and tautomeric (T) forms of PQ were optimized assuming C_s symmetry. Vertical electronic singlet and triplet excitation energies were calculated for the ground-state geometry using the TDDFT methodology at the same level of theory. Table 1 compiles the calculated and experimental data which describe the electronic absorption spectrum of PQ. Figure 2 shows the molecular orbitals involved in the description of the low-energy part of the spectrum. Two low-lying singlet states $2^1A'$ and $3^1A'$ are calculated at 3.89 and 4.00 eV, respectively. The transition to the lower state, $2^1A'$, has smaller oscillator strength and is mainly described by the highest occupied molecular orbital (HOMO) → lowest unoccupied molecular orbital (LUMO) excitation. Inspection of the corresponding orbitals reveals an internal charge transfer from the pyrrole ring to the quinoline moiety. The second, $3^1A'$, excited state is described by the HOMO−1 → LUMO main electronic configuration. In this state, some amount of electronic charge is also transferred to the quinoline part of the chromophore. The two lowest excited singlet states are characterized by a permanent dipole moment of about 4.5 D, so that the dipole moment magnitude is significantly increased compared to that

TABLE 1: TD-B3LYP/cc-pVDZ Results for Isolated PQ: Vertical Excitation Energies (eV), Oscillator Strengths (*f*), Transition Dipole Moments (*M*, D), Transition Moment Directions ($\omega(M)$, deg), Permanent Dipole Moments (μ, D), Permanent Dipole Moment Directions ($\Theta(\mu)$, deg), and Main Electronic Configurations (%)

	vertical excitation energy							main configuration[g]	
	TDDFT	expt	*f*	*M*	$\omega(M)$	μ	$\Theta(\mu)$[a]		
				Singlet States					
$1^1A'$						0.07	66.0		
$2^1A'$ ($\pi\pi^*$)	3.89 (3.52)[b]	3.66[c]	0.0197	1.15	+52.1	4.57	−1.2	H → L	85.8
								H−1 → L+1	9.1
$3^1A'$ ($\pi\pi^*$)	4.00	3.7−4.0[d]	0.0304	1.42	−10.3	4.25	10.7	H−1 → L	80.8
								H → L+1	15.0
$1^1A''$ (nπ^*)	4.64		0.0020	0.33	[f]	2.19		H−2 → L	98.7
$4^1A'$ ($\pi\pi^*$)	4.76	4.6−4.8[d]	0.0795	2.09	+69.4	3.47	1.6	H−1 → L+1	81.3
								H → L	6.8
$5^1A'$ ($\pi\pi^*$)	4.95	4.6−4.8[d]	0.4949	5.13	−6.4	2.11	−3.4	H → L+1	68.6
								H−1 → L	13.6
$2^1A''$ ($\pi\sigma^*$)	5.14		0.0020	0.30		12.38		H → L+2	95.0
$3^1A''$ ($\pi\sigma^*$)	5.25		0.0012	0.24		13.65		H−1 → L+2	94.8
$4^1A''$ (nπ^*)	5.34		0.0001	0.05	[f]	3.07		H−2 → L+1	98.3
$6^1A'$ ($\pi\pi^*$)	5.60		0.1953	3.03	13.6			H−3 → L	63.3
				Triplet States					
$1^3A'$ ($\pi\pi^*$)	2.85	2.7[e]				1.66		H → L	44.7
								H−1 → L	33.0
$2^3A'$ ($\pi\pi^*$)	3.36					4.17		H → L	40.4
								H−1 → L	52.3
$3^3A'$ ($\pi\pi^*$)	3.64					1.75		H → L+1	62.0
								H−1 → L+1	19.0
$4^3A'$ ($\pi\pi^*$)	3.82					1.55		H−1 → L+1	66.0
								H → L+1	25.7
$1^3A''$ (nπ^*)	4.08					2.19		H−2 → L	93.8

[a] See Figure 1 for angle definition. [b] The zero point corrected value for the energy gap between the $1^1A'$ and $2^1A'$ states. [c] The 0−0 absorption band in supersonic jet.[66] [d] The absorption band maxima in *n*-hexane and 1-butanol.[11] [e] The phosphorescence band maximum in 1-propanol and ethanol.[11,12,46] [f] The excited-state transition moment directed along the out-of-plane *z*-axis. [g] H, HOMO; L, LUMO.

of 0.07 D in the ground state. The excited-state transition dipole moments between the $1^1A'$ ground and the $2^1A'$ and $3^1A'$ excited states are oriented at an angle of 62.4° with respect to each other (Table 1). This analysis shows that the low-energy part of the spectrum can be assigned using Platt's nomenclature.[45] The $2^1A'$ and $3^1A'$ states correspond to Platt's ^1L_a and ^1L_b states, respectively. The low symmetry of the present system results in some state mixing and the loss of the pure identity of the transitions compared to that originally proposed by Platt; nevertheless, since this nomenclature is widely used to assign absorption spectra of indole-based chromophores, it can still be useful in the analysis of PQ. According to this nomenclature, the $4^1A'$ and $5^1A'$ states, calculated at 4.76 and 4.95 eV, correspond to Platt's ^1B_a and ^1B_b states, respectively. The ^1B_b state has the largest oscillator strength and appears as the strongest absorption band in the spectrum. Between the two pairs of the L and B states, there lies a forbidden $1^1A' \rightarrow 1^1A''$ transition, calculated at 4.64 eV (Table 1). As can be seen from the corresponding HOMO−2 and LUMO orbitals (Figure 2), this state is of nπ^* nature.

A pair of the $^1A''$ states is predicted above $4^1A'$ and $5^1A'$. In these excited states the wave function is determined by electronic excitation from HOMO or HOMO−1 to a diffuse Rydberg-type LUMO+2 orbital. The latter is of σ^* type, and it is localized on the pyrrole hydrogen atom (Figure 2). The $2^1A''$ and $3^1A''$ states can therefore be assigned to the $\pi\sigma^*$ states (Table 1). The $\pi\sigma^*$ excited states are characterized by a large excited-state dipole moment, equal to ∼12−13 D.

The calculated triplet-state manifold of PQ is also presented in Table 1. The phosphorescence spectra measured in alcohols at 77 K revealed that the lowest triplet state is located at ∼2.7 eV.[12,46] The TDDFT computed value of 2.85 eV for the lowest $1^3A'$ is in a good agreement with the experimental data. The four lowest triplet states are of $\pi\pi^*$ nature. The first nπ^* triplet state appears at 4.08 eV.

Since the calculation of the excited-state properties of PQ is carried out in the gas phase, whereas the phototautomerization occurs in polar protic solutions, it is important to assign correctly the nature of the excited state of interest. In the parent chromophore of indole, the S_1 is expected to be of ^1L_b type in the vapor phase and in nonpolar solutions, whereas in polar protic solutions the ^1L_a state is stabilized to become the lowest excited state.[47] It is also known that the ^1L_a and ^1L_b state ordering can be changed and reversed already in the vapor phase by substituents or structural modification of the indole chromophore.[48] In 7-azaindole, ^1L_a is found to be the fluorescent state even in the vapor phase according to CASSCF[49−51] and TDDFT studies.[52] It has been noted that, since in polycyclic aromatic molecules the ^1L_b state is characterized by the essential multiconfigurational character, its energy is often overestimated by such single-referenced methods as TDDFT by 0.2−0.4 eV.[53] As a result, TDDFT calculations predict correctly the energy of the $1^1A' \rightarrow {}^1L_a$ excitation, whereas they tend to overestimate the energy of the ^1L_b state. In PQ, due to strong mixing between the two lowest excited singlet states, the simple assignment to ^1L_a and ^1L_b is difficult. The $2^1A'$ and $3^1A'$ states in PQ are calculated to lie close in energy (Table 1). To verify the ordering of $2^1A'$ and $3^1A'$, the low-energy part of the spectrum was additionally calculated using the second-order coupled-cluster (RI-CC2) method.[54] This approach also predicted the same state ordering in PQ. The analysis of the nature of the $1^1A' \rightarrow 2^1A'$ excitation demonstrates that this is actually the state of interest for ESDPT. The acidic and basic properties of pyrrole and quinoline moieties become stronger upon the $1^1A' \rightarrow 2^1A'$ excitation, which provides a driving force for the proton transfer reaction.[55]

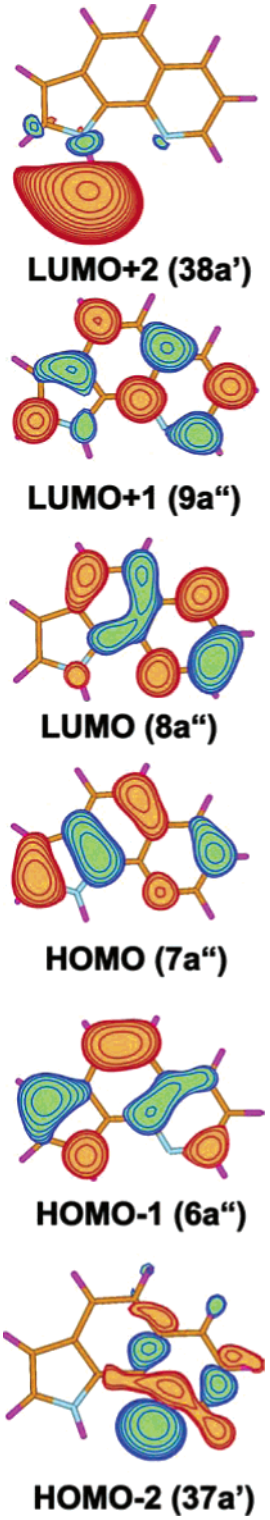

Figure 2. Molecular orbitals involved in the low-lying electronic transitions of PQ.

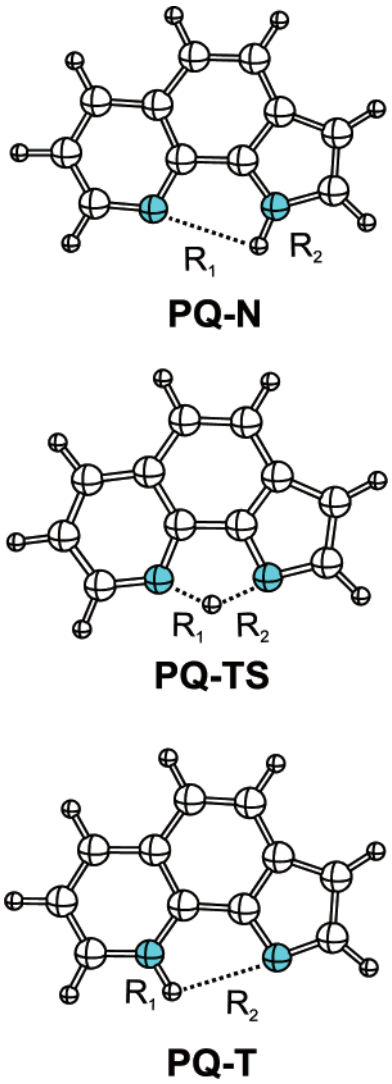

Figure 3. Optimized structures of PQ-N (top), PQ-TS (middle), and PQ-T (bottom). The two most important structural parameters, R_1 and R_2, are given in Table 2 for the S_0 and S_1 states.

To determine the profile of the potential energy path along the reaction coordinate leading from the normal (PQ-N) to the tautomeric (PQ-T) form via a transition state (PQ-TS), geometries of these three stationary points were optimized in the S_0 and S_1 states. All the stationary points were optimized assuming C_s symmetry. The corresponding structures of PQ, with the two most important structural parameters of the proton transfer path, R_1 and R_2, are shown in Figure 3. The values of R_1 and R_2 are collected in Table 2. In the normal form, the H5 proton is attached to the N4 atom of the five-membered ring, as shown in Figures 1 and 3. In the tautomer, the H5 proton is covalently bonded to the N1 atom of the six-membered quinoline-type ring. Upon passing the transition state, PQ-TS, the molecular geometry is accompanied by a large rearrangement of the aromatic ring backbone bonds relative to the PQ-N and PQ-T equilibrium structures. In the excited state, the largest change is the shortening of the N1−N4 distance from 2.87 Å in PQ-N* to 2.45 Å in PQ-TS*, respectively (an asterisk denotes structures in S_1). Table 3 contains the energetics of the proton transfer reaction. ΔE refers to the electronic energy difference between the corresponding stationary points, while ΔH_0 additionally includes the zero point vibrational energy (ΔZPE) correction term to ΔE. Table 3 also shows the relative energies with respect to the most stable structures in the S_0 and S_1 states. In the ground state, the PQ-N form is found to be the lowest energy structure. The PQ-T tautomer is calculated to be higher in energy than PQ-N by 18.6 kcal/mol (ΔH_0). The energy barrier to the intramolecular proton transfer in S_0 is equal to about 38 kcal/mol. The relative stability of PQ-N* and PQ-TS* is, however, reversed in S_1: The tautomer now becomes the most energetically stable structure, lower in energy than PQ-N* by about 16−17 kcal/mol. This clearly demonstrates that the proton transfer reaction from PQ-N* to PQ-T* is an energetically favorable process in S_1. However, in agreement with the

TABLE 2: Selected Distances (R_i, Å) and Angles (Θ_i, deg) Calculated for the Stationary Points[a] along the Proton Transfer Coordinate in PQ−$(H_2O)_n$ in the Ground State (in Parentheses) and the First Excited Singlet State

	PQ			PQ−H_2O			PQ−$(H_2O)_2$			
R_i and Θ_i	N	TS	T	N	TS	T	N	TS_a	TS_b	T
R_1	2.63	1.34	1.01	1.67	1.26	1.02	1.67	1.14	1.02	1.02
	(2.79)	(1.46)	(1.02)	(1.82)	(1.13)	(1.05)	(1.78)	(−)	(1.09)	(1.03)
R_2	1.01	1.26	2.55	1.02	1.24	1.89	1.02	1.38	1.94	1.95
	(1.01)	(1.42)	(2.54)	(0.99)	(1.42)	(1.72)	(1.00)	(−)	(1.51)	(1.84)
R_3				1.73	1.44	0.99	1.03	1.09	1.15	1.77
				(1.91)	(1.24)	(1.02)	(1.02)	(−)	(1.16)	(1.68)
R_4				1.04	1.12	1.80	1.79	1.51	1.34	1.00
				(1.02)	(1.26)	(1.67)	(1.91)	(−)	(1.16)	(1.01)
Θ_1				165.7	167.3	167.9	175.6	171.0	153.7	154.4
				(165.3)	(165.7)	(168.9)	(173.1)	(−)	(164.8)	(154.6)
Θ_2				156.1	158.7	160.1	162.1	169.1	175.3	177.4
				(158.9)	(160.8)	(160.4)	(163.8)	(−)	(175.6)	(178.9)
Θ_3							162.3	167.3	160.8	163.2
							(161.7)	(−)	(168.5)	(164.1)

[a] N, normal; TS, transition state; T, tautomer.

TABLE 3: Proton Transfer Energetics (kcal/mol) for the Calculated Stationary Points along the Proton Transfer Reaction Path in PQ−$(H_2O)_n$

		energy (kcal/mol)			
		S_0 state		S_1 state	
structure	stationary point	ΔE	ΔH_0	ΔE	ΔH_0
PQ	N	0.0	0.0	0.0	0.0
	TS	37.8		20.9	
	T	21.0	18.6	−17.2	−16.4
PQ−H_2O	N	0.0	0.0	0.0	0.0
	TS	16.1		3.0	
	T	14.6	12.7	−12.5	−11.8
PQ−$(H_2O)_2$	N	0.0	0.0	0.0	0.0
	TS_a	17.8		5.6	
	TS_b			1.5	
	T	12.8	12.6	−12.0	−11.4

spectroscopic results obtained for nonpolar and aprotic solvents, the large energy barrier makes the photoinduced proton transfer to be a process of very low probability in the isolated PQ molecule.

PQ−H_2O Complex. The effect of hydrogen bonding of water molecules on the proton transfer reaction in PQ was first studied for a 1:1 complex. To understand the dual fluorescence phenomenon, the geometries of the H-bonded complex of PQ in the normal (PQ−H_2O-N*) and tautomeric (PQ−H_2O-T*) forms were optimized in the S_1 state using the adiabatic TDDFT methodology. The geometry of transition states (PQ−H_2O-TS*) lying on the proton transfer reaction path between PQ−H_2O-N* and PQ−H_2O-T* was optimized. The stationary points were also located for the back double proton transfer cycle PQ−H_2O-N ← PQ−H_2O-T on the S_0-state surface. The structure of the corresponding stationary points is shown in Figure 4. A cyclic structure with two hydrogen bonds is found to be the most energetically stable in both PQ−H_2O-N and PQ−H_2O-T in the S_0 and S_1 states. The topology of the H-donor and H-acceptor centers of PQ favors the formation of two almost linear hydrogen bonds with very similar lengths and angles (Table 2). In S_1, the hydrogen bond is strengthened compared to S_0 in both normal and tautomer H-bonded complexes, so that the water molecule moves much closer to PQ. The transition-state structure PQ−H_2O-TS along the double proton transfer reaction coordinate was also determined in the S_0 and S_1 states as shown in Figure 4 and Table 2. Only one transition state is located along direct PQ−H_2O-N* → PQ−H_2O-T* and back PQ−H_2O-N ← PQ−H_2O-T proton transfer paths, and no other stable intermediates are found.

The tautomerization energetics is summarized in Table 3. Similarly to a bare PQ molecule, the PQ−H_2O-N form is found to be more stable in S_0. The situation is reversed after electronic excitation, so that PQ−H_2O-T* corresponds to the global energy minimum on the S_1 surface. The cyclic H-bonding with water decreases the energy difference between the normal and tautomeric structures to approximately 12−13 kcal/mol in the S_0 and S_1 states. However, a much larger effect is observed for the double proton transfer energy barrier. The formation of the cyclic 1:1 complex does not introduce steric strains in the hydrogen-bond network. This has the large effect of stabilizing the transition state. In S_1, the barrier height to double proton transfer, ΔE, is reduced to approximately 3 kcal/mol. The geometry of PQ−H_2O-TS* shows that the two protons move asynchronously. The water proton starts moving to the quinoline-type nitrogen atom before the pyrrole proton detachment is initiated, so that in PQ−H_2O-TS* this proton is found to be midway between the water oxygen and the nitrogen atom, as seen from the R_1 and R_2 distances equal to 1.26 and 1.24 Å, respectively. In the ground state, the situation is reversed. Thus the geometry of PQ−H_2O-TS is found to be closer to the tautomeric structure PQ−H_2O-T. Therefore, a rate-determining back proton transfer step is the shift of the water proton toward the nitrogen atom of the five-membered ring, as seen from the corresponding R_3 and R_4 values in Table 3. The calculations predict that the tautomerization in the 1:1 PQ−H_2O complex occurs by concerted, asynchronous double proton transfer assisted by a water molecule in both the S_0 and S_1 states. It is important to note that, contrary to the case of an isolated

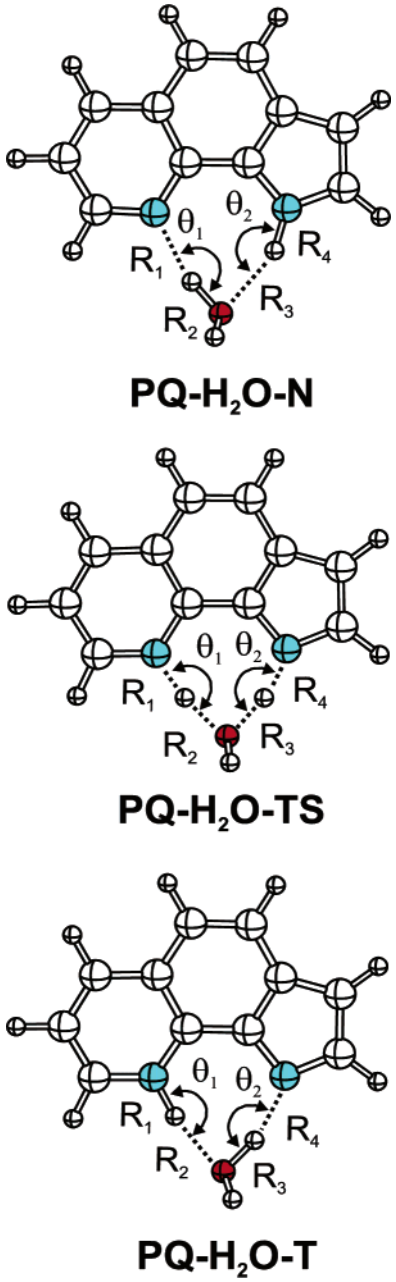

Figure 4. Optimized structures of the stationary points along the double proton transfer reaction coordinate in PQ−H_2O. The most important structural parameters are collected in Table 2.

molecule, the proton transfer through the hydrogen-bond network requires only minimal deformation of PQ skeleton upon passing the transition-state region.

The effect of hydrogen bonding with one water molecule on the photophysics of PQ is summarized in Table 4. The vertical excitation energies were calculated for S_0 and S_1 equilibrium geometries at the TD-B3LYP/cc-pVDZ level, so they correspond to electronic transitions in absorption and emission, respectively. To verify that no excited-state crossing occurs and, also, that the double proton transfer proceeds adiabatically, the corresponding excitation energies were also calculated for the transition-state structure PQ−H_2O-TS. A general trend of hydrogen bonding on the vertical excitation energies in PQ−H_2O-N compared to isolated PQ-N is that the $\pi\pi^*$ states are stabilized by approximately 0.2 eV, whereas the lowest $n\pi^*$ state is shifted to higher energy by ∼0.25 eV. The lowest singlet excitation energy of PQ−H_2O-T is calculated at 2.75 eV. This energy can be compared with the absorption maximum of 2.5 and 2.8 eV in *n*-hexane and 1-butanol for a chemical model of the PQ tautomer, in which the hydrogen atom at the quinoline nitrogen is substituted by a methyl group.[11] The two fluorescence bands of PQ in alcohol solutions are located at 3.2 and 2.1 eV, respectively.[11,12] The TDDFT values for the $S_0 \leftarrow S_1$ transition, computed at the equilibrium PQ−H_2O-N* and PQ−H_2O-T* geometries, are found to be 3.03 and 1.85 eV, respectively, about 0.2 eV below the corresponding fluorescence maxima.

PQ−$(H_2O)_2$ Complex. Different types of H-bonded solvates were found in the case of 1:2 PQ:water stoichiometry. The first group of PQ−$(H_2O)_2$ solvates has a structure similar to that of the above-described 1:1 cyclic PQ−H_2O complex. In these species the first water molecule is also cyclically H-bound to PQ, whereas the second water molecule acts as a member of the outer solvation shell, so that it attaches to the first water molecule, as either an H-bonding donor or an acceptor. Regarding the proton transfer reactivity, this set of H-bonded solvates is expected to be similar to the 1:1 cyclic PQ−H_2O complex. In terms of energy criteria, however, these PQ−$(H_2O)_2$ species are found to be less energetically stable compared to another 1:2 cyclically H-bonded solvate. The most energetically favorable 1:2 complex has the structure in which two water molecules form a cyclic H-bond chain connecting the pyrrole N−H hydrogen and the quinoline-like nitrogen atoms (Figure 5). In such an H-bonded solvate, cooperative triple proton transfer through water bridges is possible. The structure of the stationary points along a triple proton transfer reaction path in PQ−$(H_2O)_2$ is shown in Figure 5. The most important geometrical parameters of the H-bonded network are collected in Table 2.

Contrary to PQ−H_2O-N, where the two H-bonds are almost equal, the H-bond network in PQ−$(H_2O)_2$-N is characterized by some steric strain. This strain is partially reduced by out-of-plane distortions of the triple H-bond chain, so that the oxygen atom of one water molecule is shifted below the molecular plane of PQ. Upon electronic excitation to S_1, some strengthening and shortening of the H-bonding chain occurs in PQ−$(H_2O)_2$-N* (Table 2). The lengths and angles of two H-bonds formed by PQ show that in PQ−$(H_2O)_2$-N* the N···H−O bond with the quinoline-like nitrogen is more favorable than the N−H···O bond with the pyrrole moiety. The H-bonding preference is reversed in the PQ−$(H_2O)_2$-T* tautomer, so now the H-bonding with the nitrogen atom of the five-membered ring is characterized by a shorter and more linear H-bond (Figure 5). Thus, contrary to the cyclic PQ−H_2O complex, in which the H-bond lengths and angles are almost optimal to facilitate water-assisted tautomerization, a significant rearrangement of the H-bonded network is expected to occur during N* → T* proton transfer in the cyclic PQ−$(H_2O)_2$ structure.

The mechanism of proton transfer from the pyrrole to quinoline moieties through the water bridge has been studied for the PQ−$(H_2O)_2$ cyclic complex, considering the possibility of multiple proton transfer steps and transition-state structures between the PQ−$(H_2O)_2$-N* and PQ−$(H_2O)_2$-T* forms. In S_1, two transition states, TS_a* and TS_b*, along the triple proton transfer path are found (Figure 6). The first transition state, TS_a*, corresponds to highly asynchronous concerted proton movement. The three protons are shifted asynchronously along the H-bonded chain, and in TS_a* they are found to be at quite different stages of their translocation. The transfer of one proton from the water molecule to the quinoline nitrogen atom is almost complete, whereas the other two protons participating in tautomerization are still covalently bonded to the corresponding

TABLE 4: TD-B3LYP/cc-pVDZ Results for the Cyclic Complex of PQ−H_2O: Vertical Excitation Energies (eV) Corresponding to Absorption and Emission with Corresponding Oscillator Strengths (*f*)

absorption			emission		
state	vertical excitation energy	*f*	state	vertical excitation energy	*f*
		PQ−H_2O-N			
2^1A ($\pi\pi^*$)	3.71	0.0228	2^1A ($\pi\pi^*$)	3.03	0.0198
3^1A ($\pi\pi^*$)	3.82	0.0435	3^1A ($\pi\pi^*$)	3.60	0.0471
4^1A ($\pi\pi^*$)	4.60	0.0640	4^1A ($\pi\pi^*$)	4.51	0.2460
5^1A ($\pi\pi^*$)	4.82	0.4101	5^1A ($\pi\sigma^*$)	4.81	0.0017
6^1A (nπ^*)	4.90	0.0020	6^1A (nπ^*)	4.85	0.0024
7^1A ($\pi\sigma^*$)	5.07	0.0013	7^1A ($\pi\pi^*$)	4.86	0.1347
		PQ−H_2O-TS			
2^1A ($\pi\pi^*$)	3.04	0.0170	2^1A ($\pi\pi^*$)	2.65	0.0138
3^1A ($\pi\pi^*$)	3.13	0.0802	3^1A ($\pi\pi^*$)	3.30	0.0623
4^1A ($\pi\pi^*$)	4.04	0.0415	4^1A ($\pi\pi^*$)	4.29	0.1240
5^1A (nπ^*)	4.39	0.0022	5^1A ($\pi\pi^*$)	4.33	0.0467
6^1A ($\pi\pi^*$)	4.54	0.2026	6^1A (nπ^*)	4.39	0.0005
7^1A ($\pi\pi^*$)	4.58	0.0783	7^1A ($\pi\pi^*$)	4.67	0.1324
8^1A ($\pi\sigma^*$)	5.04	0.0002	8^1A ($\pi\sigma^*$)	4.96	0.0013
		PQ−H_2O-T			
2^1A ($\pi\pi^*$)	2.75	0.0100	2^1A ($\pi\pi^*$)	1.85	0.0069
3^1A ($\pi\pi^*$)	2.85	0.0983	3^1A ($\pi\pi^*$)	2.65	0.0773
4^1A ($\pi\pi^*$)	3.81	0.0364	4^1A (nπ^*)	3.76	0.0003
5^1A (nπ^*)	4.32	0.0004	5^1A ($\pi\pi^*$)	3.81	0.0876
6^1A ($\pi\pi^*$)	4.46	0.2603	6^1A ($\pi\pi^*$)	4.29	0.1161
7^1A ($\pi\sigma^*$)	4.61	0.0007	7^1A ($\pi\sigma^*$)	4.35	0.0023

heavy atoms (Table 2). In the TS_b* structure, one hydrogen atom is transferred entirely from the water cluster to the quinoline nitrogen, whereas the N−H hydrogen detachment and its movement toward the water dimer are only initiated. This difference in the sequence of the proton transfer steps in TS_a* and TS_b* can also be seen based on the corresponding R_1/R_2 and R_3/R_4 distance pairs in Table 2. The different nature of the limiting step of collective proton transfer in these transition states is also revealed by their imaginary frequency values. These values are found to be 453i and 3397i cm^{-1} for TS_a* and TS_b*, respectively. The detailed structure and high amplitude motions of the protons involved in the proton transfer process are shown in Figure 6. It is also interesting to consider the energetics of both transition states. The ΔE energy barrier between the PQ−$(H_2O)_2$-N* form and the corresponding transition states is calculated to be 5.6 and 1.5 kcal/mol for TS_a* and TS_b*, respectively.

The analysis of geometry and energetics of the two TS_a* and TS_b* transition states suggests that in the PQ−$(H_2O)_2$ complex the complete tautomerization does not occur by a mechanism of simultaneous and cooperative movement of the three protons along the H-bond network connecting the H-bond donor and acceptor groups of PQ. This mechanism assumes cooperative breaking and re-forming of the three H-bonds. Such concerted H-bond reorganization can, in principle, be expected for water bridges connected by equivalent or similar H-bonds.[56−59] In PQ−$(H_2O)_2$-N*, the significant nonequivalence of H-bonds causes strong asynchronicity in the collective proton movement. This leads to the situation where only one H-bond is being broken along the cyclic H-bond network so that, overall, the energy barrier for the proton transfer is reduced. Such behavior can cause the triple proton transfer process to occur by the stepwise mechanism, so proton transfer can occur in two steps through the TS_a* and TS_b* transition states. In the first step, one proton is transferred from the water dimer to the quinoline nitrogen, whereas in the second stage the N−H proton is detached and translocated to the nearest water oxygen. The first step, which is higher in energy, should be rate-determining.

Still, this mechanism leaves several open questions. First, as can be seen from the corresponding transition-state structures in Figure 6, a rapid proton hopping should also occur between the two oxygen atoms of the water dimer during the H-bond network rearrangement taking place along the reaction path TS_a* → TS_b*. Second, a local energy minimum should exist between the TS_a* and TS_b* transition states on the S_1 hypersurface. However, no other stable excited-state intermediate could be optimized in the region of the S_1 hypersurface between the TS_a* and TS_b* energy maxima. This is mainly because the TDDFT excited-state optimization procedure encountered a wave function instability. Further rearrangement of the H-bond network along the TS_a* → TS_b* path resulted in the appearance of spurious solvent−solute charge transfer excitations, so that the TDDFT excited-state optimization procedure was becoming unstable due to a decrease of the HOMO−LUMO energy gap of the system. This deficiency in the TDDFT methodology has been reported for solvated acetone studied by ab initio molecular dynamics methods.[60,61] In this aqueous system, thermal fluctuation and the water O−H bond stretching resulted also in the broadening of the HOMO energy of the solvated system due to mixing of the HOMO of the studied chromophore with the corresponding occupied orbitals of the solvent. This orbital mixing results in the appearance of charge transfer excitations with nonnegligible solvent character.

The effect of the second solvation shell on the phototautomerization in the cyclic PQ−$(H_2O)_2$ complex was studied by adding extra water molecules, up to PQ:water stoichiometries of 1:6. These results demonstrated that the appearance of the two TS_a* and TS_b* transition states along the triple proton transfer path in the 1:2 complex may be partially induced by a lack of proper solvation, so that in the larger solvates the cooperative proton movement of the three protons can still occur through one transition state. However, this process requires significant rearrangement of H-bond bridges and, as a result, higher activation energies of about 5−6 kcal/mol are needed.

Discussion and Conclusions

Fluorescence spectra of PQ are characterized by a single emission band and quite high quantum yields of about 0.25 and 0.16 in nonpolar (*n*-hexane) and polar aprotic (acetonitrile)

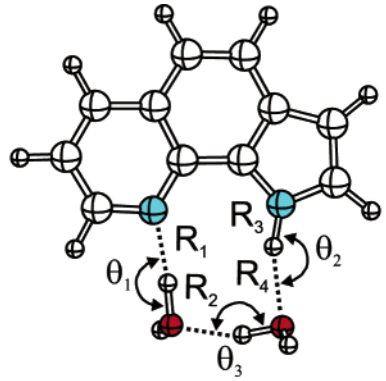

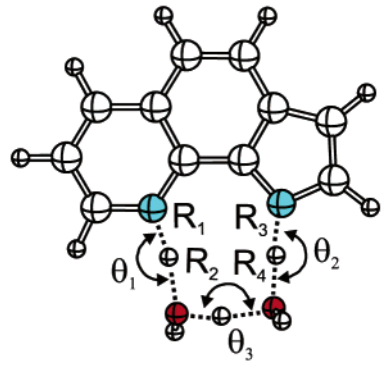

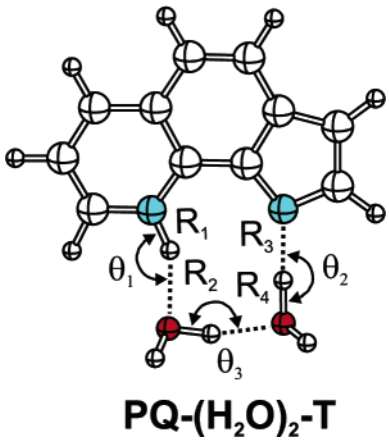

Figure 5. Optimized structures of the stationary points along the triple proton transfer reaction coordinate in the cyclic PQ−$(H_2O)_2$ complex. The most important structural parameters are collected in Table 2.

media, respectively.[11] In alcohol and water solutions the fluorescence quantum yield becomes very weak. The most interesting finding is that dual fluorescence is observed in these solvents. In addition to the first "normal" (F_1) band, similar in the spectral position to the emission observed in polar aprotic solvents, another (F_2) band appears at lower energy. The latter has been attributed to the fluorescent product of double proton tautomerization occurring in a photoexcited cyclically H-bonded complex of PQ with solvent molecules. The electron density redistribution between the pyrrole and quinoline rings occurring upon excitation is expected to be the driving force for the excited-state tautomerization. An increase of the excited-state pK_a of the acceptor quinoline nitrogen atom and a decrease of the corresponding pK_a of the donor NH group were found to be $\Delta pK_a(N) = 9.6$ and $\Delta pK_a(NH) = -6.0$, respectively.[11] In addition to steady-state fluorescence analysis, subpicosecond time-resolved fluorescence transient measurements have shown that the F_1 band contains two fast decay components with time constants of $\tau_1 = 0.6-0.9$ ps and $\tau_2 = 6-11$ ps, and a slower decay component, τ_3, with a time constant between 50 and 150 ps, depending on the alcohol.[17] On the other hand, the F_2 band reveals a fast biexponential rise occurring at the same rate as the fast initial decay of the F_1 emission; no rise time corresponding to the slow decay of F_1 has been detected. These experiments provided independent additional evidence that the F_1 and F_2 emission bands originate from different species. The two fast time components, τ_1 and τ_2, observed in the decay of F_1 and the rise of F_2 have been attributed to the presence of two distinct cyclic H-bonded complexes of PQ with solvent molecules that may differ slightly in H-bond configurations; however, both of these species are able to undergo solvent-assisted proton transfer. Such a kinetic scheme supposes that rapid multiple proton movements occur in a one-step process and no intermediate species are formed. The longer lived decay component τ_3 of the F_1 band has therefore been assigned to solute−solvent H-bonded complexes not involved in a fast excited-state proton transfer. The decay components τ_1 and τ_2 revealed weak temperature and viscosity dependences, in contrast to a strong dependence observed for τ_3. The F_2 emission could be observed even in glassy alcoholic solutions of PQ at 123 K, where solvent relaxation is blocked.[46] Thus, cyclic

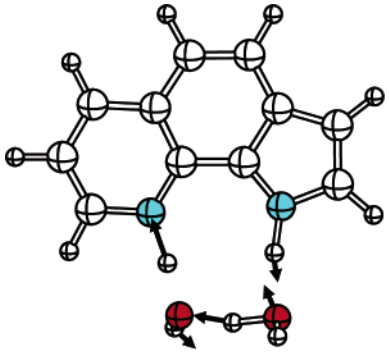

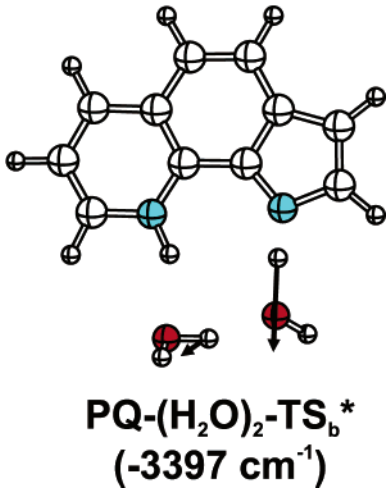

Figure 6. Structures of two transition states TS_a* and TS_b* on the triple proton transfer reaction path in the cyclic PQ−$(H_2O)_2$ complex.

H-bonded species, with appropriately solvated structure for a proton transfer reaction, are formed already in the ground state, so they do not require large solvent relaxation around an excited chromophore. Only when such a relaxation process is enabled in liquid solution at higher temperatures does an additional component appear, corresponding to the decay time τ_3 of the F_1 emission. Since this component has no counterpart in the corresponding rise of the F_2 emission, the decay characterized by τ_3 corresponds to internal conversion from the photoexcited chromophore to its ground state.

The DFT calculations correctly predict the existence of both kinds of complexes in bulk water solution. The ground-state binding energies, corrected for basis set superposition errors, are found to be −9.3 and −12.6 kcal/mol for the PQ−H_2O and PQ−$(H_2O)_2$ complexes, respectively. One should note that the latter value includes a contribution of water−water hydrogen bonding. The calculation for a water dimer using the same model and basis set yielded −2.6 kcal/mol as the hydrogen-bond energy.

The adiabatic TDDFT calculations demonstrate that the $S_0 \rightarrow S_1$ excitation of the isolated molecule of PQ is accompanied by significant intramolecular transfer of electron density from the pyrrole ring to the quinoline fragment, so that the acidity of the N−H group and the basicity of the quinoline moiety are increased. Thus, in agreement with experiment, the proton transfer photoreactivity of the S_1 state is found to be higher than that of S_0. The phototautomeric form with the hydrogen atom attached to the quinoline nitrogen is found to be adiabatically more stable with respect to the initially excited normal form by approximately 17 kcal/mol (Table 3). However, the topology of the H-donor and acceptor centers in PQ is not favorable for the intramolecular proton transfer due to the large energy barrier of about 21 kcal/mol separating the normal N* and tautomer T* forms. In the cyclic, H-bonded complexes of PQ with one or two water molecules, the energy barrier for proton transfer is dramatically decreased, so the tautomerization can, in principle, occur in both PQ−H_2O and PQ−$(H_2O)_2$ solvates. The cyclic PQ−H_2O-N complex is characterized by a well-defined, rigidly H-bonded structure with the two almost equivalent H-bonds. Upon excitation of such a complex, the tautomerization can occur rapidly in one step as a concerted asynchronous movement of the two protons. This process is expected to be almost barrierless, and it does not require a large rearrangement of the positions of heavy atoms upon passing the transition-state region. Thus, the excited-state proton transfer in this solvate can occur in frozen solutions at low temperatures. In contrast to the cyclic PQ−H_2O structure, the cyclic PQ−$(H_2O)_2$ solvate is affected by steric strain and unfavorable H-bond arrangement. Therefore, some extra activation energy is needed for initiating the proton dislocation along the H-bond network. For the same reason, the transfer of protons is also found to be highly asynchronous, so large relaxation and reorganization of the water dimer including some translations and rotations of two oxygen atoms of the water molecules are required during the proton translocation from the pyrrole H atom to the quinoline nitrogen. The PQ−$(H_2O)_2$ complex can be viewed as an intermediate form between PQ−H_2O and noncyclic poly-H-bonded aggregates in bulk solvent. Therefore, the reaction coordinate along the H-bond network can be further perturbed in the PQ−$(H_2O)_2$ complex solvated by bulk H-bonded solvent during H-bond breaking and re-forming dynamics. As a result, H-bonding dynamics is able to induce nonradiative deactivation of the excited chromophore of PQ via a mechanism different from that of the excited-state proton transfer. For some unfavorable H-bonding configurations the N−H bond stretching as an initial stage followed by proton movement to the qunoline acceptor center may initiate migration of the corresponding hydrogen atom to the surrounding solvent molecules instead of being transferred to the quinoline nitrogen atom. This mechanism of the photodetachment of the hydrogen atom from the NH group of pyrrole-containing chromophores, driven by a repulsive $^1\pi\sigma^*$ state, has recently been proposed and experimentally confirmed.[40,62−65] Thus, the H-bonding dynamics around the excited chromophore of PQ induced by proton movement from the pyrrole NH atom to the qunoline nitrogen center might potentially switch the proton transfer reaction to the reaction of the photodetachment of the NH hydrogen atom to bulk solvent.

Acknowledgment. A.K. acknowledges support from the EC Grant G5MA-CT-2002-04026.

References and Notes

(1) Taylor, C. A.; El-Bayoumi, M. A.; Kasha, M. *Proc. Natl. Acad. Sci. U.S.A.* **1969**, *63*, 253.
(2) Waluk, J.; Grabowska, A.; Pakuła, B.; Sepioł, J. *J. Phys. Chem.* **1984**, *88*, 1160.
(3) Waluk, J.; Komorowski, S. J.; Herbich, J. *J. Phys. Chem.* **1986**, *90*, 3868.
(4) Kwon, O.-H.; Lee, Y.-S.; Park, H. J.; Kim, Y.; Jang, D.-J. *Angew. Chem., Int. Ed.* **2004**, *43*, 5792.
(5) Moog, R. S.; Maroncelli, M. *J. Phys. Chem.* **1991**, *95*, 10359.
(6) Takeuchi, S.; Tahara, T. *J. Phys. Chem. A* **1998**, *102*, 7740.
(7) Sakota, K.; Okabe, C.; Nishi, N.; Sekiya, H. *J. Phys. Chem. A* **2005**, *109*, 5245.
(8) Chou, P. T. *J. Chin. Chem. Soc.* **2001**, *48*, 651.
(9) Smirnov, A. V.; English, D. S.; Rich, R. L.; Lane, J.; Teyton, L.; Schwabacher, A. W.; Luo, S.; Thornburg, R. W.; Petrich, J. W. *J. Phys. Chem. B* **1997**, *101*, 2758.
(10) Herbich, J.; Dobkowski, J.; Thummel, R. P.; Henge, V.; Waluk, J. *J. Phys. Chem. A* **1997**, *101*, 5839.
(11) Kyrychenko, A.; Herbich, J.; Izydorzak, M.; Wu, F.; Thummel, R. P.; Waluk, J. *J. Am. Chem. Soc.* **1999**, *121*, 11179.
(12) Del Valle, J. C.; Dominguez, E.; Kasha, M. *J. Phys. Chem. A* **1999**, *103*, 2467.
(13) Waluk, J. *Acc. Chem. Res.* **2003**, *36*, 832.
(14) Kijak, M.; Zielińska, A.; Thummel, R. P.; Herbich, J.; Waluk, J. *Chem. Phys. Lett.* **2002**, *366*, 329.
(15) Kyrychenko, A.; Stepanenko, Y.; Waluk, J. *J. Phys. Chem. A* **2000**, *104*, 9542.
(16) Mente, S.; Maroncelli, M. *J. Phys. Chem. A* **1998**, *102*, 3860.
(17) Marks, D.; Zhang, H.; Borowicz, P.; Waluk, J.; Glasbeek, M. *J. Phys. Chem. A* **2000**, *104*, 7167.
(18) Gordon, M. S. *J. Phys. Chem.* **1996**, *100*, 3974.
(19) Chaban, G. M.; Gordon, M. S. *J. Phys. Chem. A* **1999**, *103*, 185.
(20) Nakajima, A.; Hirano, M.; Hasumi, R.; Kaya, K.; Watanabe, H.; Carter, C. C.; Williamson, J. M.; Miller, T. A. *J. Phys. Chem. A* **1997**, *101*, 392.
(21) Yokoyama, H.; Watanabe, H.; Omi, T.; Ishiuchi, S.; Fujii, M. *J. Phys. Chem. A* **2001**, *105*, 9366.
(22) Smedarchina, Z.; Siebrand, W.; Fernández-Ramos, A.; Gorb, L.; Leszczynski, J. *J. Chem. Phys.* **2000**, *112*, 566.
(23) Fernández-Ramos, A.; Smedarchina, Z.; Siebrand, W.; Zgierski, M. Z. *J. Chem. Phys.* **2001**, *114*, 7518.
(24) Casadesús, R.; Moreno, M.; Lluch, J. M. *Chem. Phys.* **2003**, *290*, 319.
(25) Li, Q.-S.; Fang, W.-H.; Yu, J. G. *J. Phys. Chem. A* **2005**, *109*, 3983.
(26) Hu, X.; Li, H.; Liang, W.; Han, S. *J. Phys. Chem. B* **2005**, *109*, 5935.
(27) Chou, P.-T.; Wei, C.-Y.; Wang, C.-R. C.; Hung, F.-T.; Chang, C.-P. *J. Phys. Chem. A* **1999**, *103*, 1939.
(28) Fang, W.-H. *J. Am. Chem. Soc.* **1998**, *120*, 7568.
(29) Kohtani, S.; Tagami, A.; Nakagaki, R. *Chem. Phys. Lett.* **2000**, *316*, 88.
(30) Fang, W.-H. *J. Phys. Chem. A* **1999**, *103*, 5567.
(31) Meuwly, M.; Bach, A.; Leutwyler, S. *J. Am. Chem. Soc.* **2001**, *123*, 11446.
(32) Manca, C.; Tanner, C.; Coussan, S.; Bach, A.; Leutwyler, S. *J. Chem. Phys.* **2004**, *121*, 2578.

(33) Tanner, C.; Thut, M.; Steinlin, A.; Manca, C.; Leutwyler, S. *J. Phys. Chem. A* **2006**, *110*, 1758.
(34) Coussan, S.; Meuwly, M.; Leutwyler, S. *J. Chem. Phys.* **2001**, *114*, 3524.
(35) Tanner, C.; Manca, C.; Leutwyler, S. *J. Chem. Phys.* **2005**, *122*, 204326.
(36) Furche, F.; Ahlrichs, R. *J. Chem. Phys.* **2002**, *117*, 7433.
(37) Kohn, W.; Sham, L. J. *Phys. Rev.* **1965**, *140*, A1133.
(38) Dunning, T. H., Jr., *J. Chem. Phys.* **1989**, *90*, 1007.
(39) Serrano-Andrés, L.; Roos, B. O. *J. Am. Chem. Soc.* **1996**, *118*, 185.
(40) Sobolewski, A. L.; Domcke, W. *Chem. Phys. Lett.* **1999**, *315*, 293.
(41) Becke, A. D. *J. Chem. Phys.* **1993**, *98*, 5648.
(42) Haettig, C.; Weigend, F. *J. Chem. Phys.* **2000**, *113*, 5154.
(43) Haettig, C.; Koehn, A. *J. Chem. Phys.* **2002**, *117*, 6939.
(44) Ahlrichs, R.; Bär, M.; Häser, M.; Hom, H.; Kölmel, C. *Chem. Phys. Lett.* **1989**, *162*, 165.
(45) Platt, J. R. *J. Chem. Phys.* **1949**, *17*, 484.
(46) Kyrychenko, A.; Herbich, J.; Izydorzak, M.; Gil, M.; Dobkowski, J.; Wu, F.; Thummel, R. P.; Waluk, J. *Isr. J. Chem.* **1999**, *39*, 309.
(47) Catalán, J.; Dìaz, C. *Chem. Phys. Lett.* **2003**, *368*, 717.
(48) Muiño, P. L.; Callis, P. R. *J. Chem. Phys.* **1994**, *100*, 4093.
(49) Borin, A. C.; Serrano-Andrés, L. *Chem. Phys.* **2000**, *262*, 253.
(50) Serrano-Andrés, L.; Borin, A. C. *Chem. Phys.* **2000**, *262*, 267.
(51) Serrano-Andrés, L.; Merchán, M.; Borin, A. C.; Stålring, J. *Int. J. Quantum Chem.* **2001**, *84*, 181.
(52) Catalán, J.; de Paz, J. L. G. *J. Chem. Phys.* **2005**, *122*, 244320.
(53) Parac, M.; Grimme, S. *J. Phys. Chem. A* **2002**, *106*, 6844.
(54) Hättig, C.; Köhn, A. *J. Chem. Phys.* **2002**, *117*, 6939.
(55) Catalán, J. *J. Am. Chem. Soc.* **2001**, *123*, 11940.
(56) Kornyshev, A. A.; Kuznetsov, A. M.; Spohr, E.; Ulstrup, J. *J. Phys. Chem. B* **2003**, *107*, 3351.
(57) Agmon, N. *J. Phys. Chem. A* **2005**, *109*, 13.
(58) Lapid, H.; Agmon, N.; Petersen, M. K.; Voth, G. A. *J. Chem. Phys.* **2005**, *122*, 014506.
(59) Mezer, A.; Friedman, R.; Noivirt, O.; Nachliel, E.; Gutman, M. *J. Phys. Chem. B* **2005**, *109*, 11379.
(60) Bernasconi, L.; Sprik, M.; Hutter, J. *J. Chem. Phys.* **2003**, *119*, 12417.
(61) Bernasconi, L.; Sprik, M.; Hutter, J. *Chem. Phys. Lett.* **2004**, *394*, 141.
(62) Sobolewski, A. L.; Domcke, W. *Chem. Phys. Lett.* **2000**, *321*, 479.
(63) Sobolewski, A. L.; Domcke, W. *Chem. Phys. Lett.* **2000**, *329*, 130.
(64) Sobolewski, A. L.; Domcke, W. *Chem. Phys.* **2000**, *259*, 181.
(65) Sobolewski, A. L.; Domcke, W.; Dedonder-Lardeux, C.; Jouvet, C. *Phys. Chem. Chem. Phys.* **2002**, *4*, 1093.
(66) Nosenko, Y.; Herbich, J.; Kyrychenko, A.; Gorski, A.; Brutschy, B.; Waluk, J. Manuscript in preparation.